

Ammonolysis of Tantalum Alkyls: Formation of Cubic TaN and a Trimeric Nitride, [Cp*MeTaN]₃

Mark M. Banaszak Holl, Meinolf Kersting, Bradford D. Pendley, and Peter T. Wolczanski*[†]

Received August 10, 1989

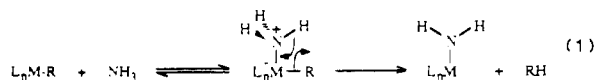
Ammonolyses of precursor alkyl complexes have been employed to generate nitrides of tantalum. Treatment of (^tBuCH₂)₃Ta=CH^tBu (**1**) with NH₃ led to the formation of an orange precipitate, best formulated as an oligomer, [TaN_{2.14}H_{1.35}]_n (**2**), on the basis of ammonia uptake, neopentane loss, and combustion analysis. Upon thermolysis of **2** at 400 °C (24 h), a ~6% weight loss occurred and amorphous TaN was generated; crystalline cubic TaN (*Fm*3*m*, 95%) was formed after further heating at 820 °C (3 days). Under ambient light, a similar ammonolysis of **1** afforded another oligomer, [TaC_{1.41}H_{3.96}N_{1.90}]_n (**2'**); thermolysis of **2'** (400 °C, 24 h) resulted in a ~14% weight loss and amorphous TaN that was subsequently annealed to pure, crystalline cubic TaN (820 °C, 3 days, XRD, *Fm*3*m*). Cp*TaMe₄ (**3**, Cp* = η⁵-C₅Me₅) was exposed to excess NH₃ in order to model the ammonolysis process. The uptake of 1 equiv of ammonia/equiv of Ta was noted, 3 equiv of CH₄ was released, and [Cp*MeTaN]₃ (**4**) formed in 90% yield. Cyclic trimer **4** contains equivalent TaN distances (1.887 (17) Å) akin to those of related phosphazenes. Crystal data: monoclinic, *P*2₁/*c*, *a* = 16.951 (5) Å, *b* = 8.920 (3) Å, *c* = 23.141 (6) Å, β = 91.47 (2)°, *Z* = 4, *T* = -100 °C. EHMO calculations revealed why a structure containing alternating double and single TaN bonds was not favored. The low-lying LUMO of **4** was predicted to be nonbonding; consequently, **4** was reduced with Na/K to yield [K·nEt₂O]⁺[Cp*MeTaN₃]⁻ (**5**). A reversible reduction wave at *E*^o = -2.5 V vs SSCE was also observed. Similar IR spectra of **4** (ν(TaN-Ta) = 960 cm⁻¹) and **5** (ν(TaN-Ta) = 964 cm⁻¹) support the contention that the LUMO is nonbonding. The relationship of **4** to the solid-state nitrides produced via ammonolysis is addressed.

Introduction

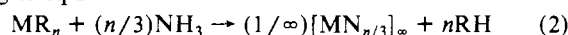
A burgeoning discipline of transition-metal inorganic and organometallic chemistry involves the preparation of solid-state materials via solution methods using molecular precursors.^{1–5} Conventional thermal techniques that typically result in thermodynamically determined products can be circumvented by using this approach. Potential advantages of such procedures include the discovery of low-temperature routes to known solids,^{6–8} the generation of intermediate oligomers or polymers^{9–11} that can be processed with greater efficiency, the utilization of complex, yet volatile, compounds for chemical vapor deposition (CVD),¹² and the synthesis of new, kinetically stable materials.

Refractory metal nitrides, a class of materials possessing interesting physical and electronic properties, are limited in scope with respect to related oxides, perhaps as a consequence of the severe conditions (e.g., *T* > 1000 °C) used in standard preparative procedures.¹³ From this standpoint, the development of solution syntheses to M_xN_y solids via inorganic⁸ or organometallic precursors represents an intriguing challenge in the materials field. Reported herein are initial efforts based on the ammonolysis of metal alkyls, including a model study that resulted in the formation of a trimeric nitride, [Cp*MeTaN]₃ (Cp* = η⁵-C₅Me₅).^{14,15} With this method, a standard thermal process for the formation of cubic TaN (*Fm*3*m*)¹⁶ was discovered. This phase has been previously prepared under relatively extreme conditions.^{17–22}

The ready availability and highly reactive nature of ammonia renders this small molecule attractive as a nitrogen source. Early metal alkyl bonds, polarized M^{δ+}-R^{δ-}, were considered probable functionalities for ammonolyses.²³ A bound NH₃ is expected to possess acidic hydrogens, thus the 1,2-alkane elimination^{23,24} in eq 1 may be viewed as a deprotonation by an anionic alkyl. In



addition to these kinetic arguments, the formation of strong metal–nitrogen bonds, both σ and π, and the entropically favorable release of several equivalents of alkane provide a strong thermodynamic preference for the formation of metal nitrides according to eq 2.



Results

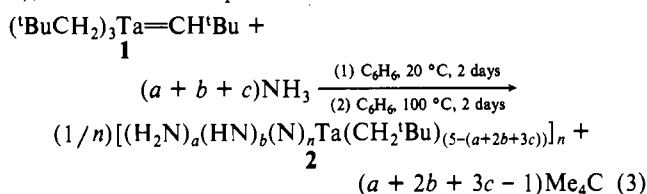
TaN from Ammonolysis. In accord with the above arguments, a thermally stable polyalkyl, (^tBuCH₂)₃Ta=CH^tBu (**1**),²⁵ was

chosen as a precursor to tantalum nitride. Treatment of **1** with excess ammonia (~5 equiv) in benzene at 20 °C, followed by

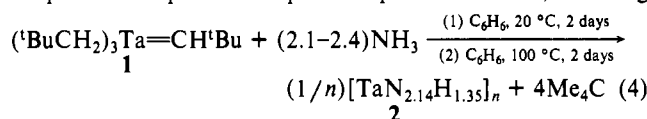
- (1) Parshall, G. W. *Organometallics* **1987**, *6*, 687–692.
- (2) (a) Wynne, K. J.; Rice, R. W. *Annu. Rev. Mater. Sci.* **1984**, *14*, 297–334. (b) Rice, R. W. *Am. Ceram. Soc. Bull.* **1983**, *62*, 889–892.
- (3) (a) Robinson, A. L. *Science* **1986**, *233*, 25–27. (b) *Sci. Am.* **1986**, *255*, 50–203. (c) Canby, T. Y.; O'Rear, C. *Natl. Geogr.* **1989**, *176*, 746–781.
- (4) (a) Hench, L. L.; Ulrich, D. R., Eds. *Ultrastructure Processing of Ceramics, Glasses and Composites*; John Wiley & Sons: New York, 1983. (b) Brinker, C. J.; Clark, D. E.; Ulrich, D. R., Eds. *Better Ceramics Through Chemistry*; North-Holland: New York, 1984.
- (5) Laine, R. M., Ed. *Transformation of Organometallics into Common and Exotic Materials: Design and Activation*; NATO Advanced Science Institute Series; Martinus Nijhoff: Dordrecht, The Netherlands, 1988.
- (6) (a) Martin, M. J.; Qiang, G.-H.; Schleich, D. M. *Inorg. Chem.* **1988**, *27*, 2804–2808. (b) Czekaj, C. L.; Rau, M. S.; Geoffroy, G. L.; Guiton, T. A.; Pantano, C. G. *Inorg. Chem.* **1988**, *27*, 3267–3269.
- (7) Czekaj, C. L.; Geoffroy, G. L. *Inorg. Chem.* **1988**, *27*, 8–10.
- (8) (a) Brown, G. M.; Maya, L. *J. Am. Ceram. Soc.* **1988**, *80*, 78–82. (b) Maya, L. *Inorg. Chem.* **1987**, *26*, 1459–1462. (c) Maya, L. *Inorg. Chem.* **1986**, *25*, 4213–4217. (d) Bradley, D. C.; Hursthouse, M. B.; Abdul Malik, K. M.; Nielson, A. J.; Chota Vuru, G. B. *J. Chem. Soc., Dalton Trans.* **1984**, 1069–1075 and references therein.
- (9) (a) Roesky, H. W.; Lücke, M. *J. Chem. Soc., Chem. Commun.* **1989**, 748. (b) Roesky, H. W.; Lücke, M. *Angew. Chem.* **1989**, *101*, 480.
- (10) Critchlow, S. C.; Lerchen, M. E.; Smith, R. C.; Doherty, N. M. *J. Am. Chem. Soc.* **1988**, *110*, 8071–8075.
- (11) (a) Willing, W.; Christophersen, R.; Müller, U.; Dehnicke, K. *Z. Anorg. Allg. Chem.* **1987**, *555*, 16–22. (b) Chan, D. M.-T.; Chisholm, M. H.; Folting, K.; Hoffman, J. C.; Marchant, N. S. *Inorg. Chem.* **1986**, *25*, 4170–4174.
- (12) (a) Gozum, J. E.; Pollina, D. M.; Jensen, J. A.; Girolami, G. S. *J. Am. Chem. Soc.* **1988**, *110*, 2688–2689. (b) Jensen, J. A.; Gozum, J. E.; Pollina, D. M.; Girolami, G. S. *J. Am. Chem. Soc.* **1988**, *110*, 1643–1644. (c) Girolami, G. S.; Jensen, J. A.; Pollina, D. M.; Williams, W. S.; Kaloyeros, A. E.; Allocca, C. M. *J. Am. Chem. Soc.* **1987**, *107*, 1579–1580. (d) Kaloyeros, A. E.; Williams, W. S.; Allocca, C. M.; Pollina, D. M.; Girolami, G. S. *Adv. Ceram. Mater.* **1987**, *2*, 257–263 and references therein.
- (13) (a) Toth, L. E. *Transition Metal Carbides and Nitrides*; Academic Press: New York, 1971. (b) Johansen, H. A. In *Recent Developments in the Chemistry of Transition Metal Carbides and Nitrides*; Scott, A. F., Ed.; Survey of Progress in Chemistry 8; Academic Press: New York, 1977.
- (14) For a review of molecular nitrides, see: Dehnicke, K.; Strähle, J. *Angew. Chem., Int. Ed. Engl.* **1981**, *20*, 413–426.
- (15) For a perspective of the metal nitride bond, see: Nugent, W. A.; Mayer, J. M. *Metal-Ligand Multiple Bonds*; John Wiley & Sons: New York, 1988.
- (16) Politis, C. *Contemporary Inorganic Materials Proceedings of the German-Yugoslav Meeting on Materials Science and Development, 3rd*; Petzow, G., Huppmann, W. J., Eds.; Dr. Riederer-Verlag GmbH: Stuttgart, FRG, 1978; pp 152–157.
- (17) Gerstenberg, D.; Hall, P. M. *J. Electrochem. Soc.* **1964**, *111*, 936–942.
- (18) (a) Boiko, L. G.; Popova, S. V. *JETP Lett.* **1970**, *12*, 70–71. (b) Kieffer, R.; Ettmayer, P.; Freundhofmeier, M.; Gatterer, J. *Monatsh. Chem.* **1971**, *102*, 483–485.

[†] Alfred P. Sloan Foundation Fellow, 1987–1989.

thermolysis at 100 °C, resulted in the uptake of NH₃ (~2.4 equiv = a + b + c), a complimentary loss of neopentane (~3.9 equiv by ¹H NMR), and the precipitation of an amorphous orange precipitate over the course of 4 days.²⁶ A generic equation for the multistep thermal sequence leading to the presumed oligomer, [(H₂N)_a(HN)_b(N)_cTa(CH₂^tBu)_{(5-(a+2b+3c))}]_n (**2**; a + 2b + 3c ≥ 1), is illustrated in eq 3.

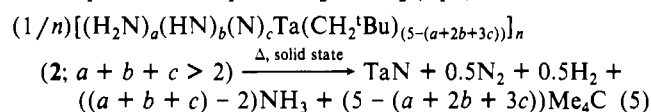


Combustion analyses of **2** (e.g., found (av): C, 1.53; H, 0.91; N, 13.89; TaC_{0.28}N_{2.16}H_{1.28}) revealed a minimal amount of carbon,²⁷ presumably still bound as neopentyl groups, and therefore were in general agreement with the loss of nearly 4 equiv of neopentane. Equation 4 depicts a representative run, assuming



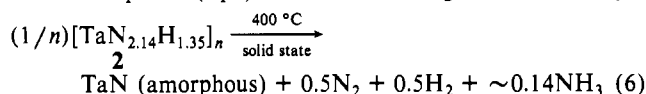
total neopentane loss. Subtracting out the carbon and an appropriate amount of hydrogen (5:11 C:H) allowed a rough elemental composition of TaN_{2.14}H_{1.35} to be obtained for **2**. The formulation was encouraging since the nitrogen component approached the NH₃/Ta uptake number. The small discrepancy (~0.2 N) could be due to a small amount of ammonia initially trapped in the orange powder. Assuming the tantalum in **2** exists as Ta(V), a substantial number of nitrido ligands must be present in the oligomer, since the N:H ratio is 1.59. The lowest N:H ratio for nitrogen to be present in only imido or amido ligands is 0.75. Unfortunately, the relative number of amido, imido, and nitrido ligands cannot be determined from the analytical methods utilized,²⁸ and the IR spectrum of **2** was uninformative.

Provided **2** (a + b + c > 2) contains only Ta(V) and no N-N bonds, stoichiometry requires that its thermolysis to give the known Ta^{III}N produce 0.5 equiv of H₂ and N₂ (eq 5). The amount of



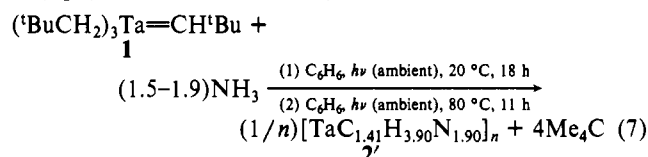
ammonia released is equal to (a + b + c) - 2, and all CH₂^tBu groups are lost as neopentane; thus, the oxidation of bound nitrogen to N₂ is responsible for the corresponding reduction of the tan-

talum. A solid orange sample of **2** incurred a ~6% weight loss after thermolysis at 400 °C for 24 h, somewhat less than the 9.7% predicted for TaC_{0.28}N_{2.16}H_{1.28}, but closer to the 8.2% loss anticipated for TaN_{2.14}H_{1.35}. If amorphous TaN is the product, the loss of ~0.5 equiv each of H₂ and N₂, and 0.14 equiv of NH₃ would be expected (eq 6). Further annealing at 820 °C (3 days)



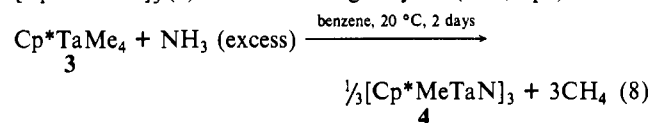
produced a jet-black solid that developed a grayish cast upon exposure to air. X-ray powder diffraction studies indicated that the sample was ~95% cubic (*Fm3m*) TaN and ~5% TaO.^{29,30} At higher annealing temperatures (>900 °C; 3 days), TaN_{0.8}^{18,31} was observed to grow in with a corresponding weight loss.

Interestingly, the conversion of (^tBuCH₂)₃Ta=CH^tBu (**1**) to oligomer **2** is complicated by photochemical events. Treatment of **1** with 2.0 equiv of NH₃ in benzene at 20 °C in ambient light afforded a green-orange precipitate after 18 h. After the mixture was heated for 11 h at 80 °C, analysis of the reaction revealed an uptake of 1.5 equiv of NH₃, the loss of 3.7 equiv of neopentane, and the formation of a green-orange powder, **2'**.³² It is conceivable that this darker precipitate has incurred some reduction, possibly via a photochemically induced elimination of neopentyl groups from the Ta centers. Combustion analysis indicated that oligomer **2'** (eq 7) contained considerably more carbon (found: C, 7.41;



H, 1.72; N, 11.65; TaC_{1.41}H_{3.90}N_{1.90});²⁷ again assuming all carbon is present as CH₂^tBu groups, there is still approximately a 1:3.5 CH₂^tBu:Ta ratio contrasting sharply with **2**, where the CH₂^tBu:Ta ratio was 1:18. The uptake of ~1.5 NH₃ by **1** deviates somewhat from the 1.9 equiv predicted by the combustion analysis. A ~14% weight loss was observed upon thermolysis of a solid green-orange sample of **2'** at 400 °C for 24 h, consistent with the expected stoichiometric loss (14.6%) from TaC_{1.41}H_{3.90}N_{1.90}. Further annealing at 820 °C (3 days) produced a jet-black solid that did not appear affected by exposure to air. X-ray powder diffraction indicated that cubic TaN (*Fm3m*) was the only species present.^{21,29} Further attempts to understand the nature of potentially useful photolytic processing methods are ongoing.

[Cp*MeTaN]₃ from Ammonolysis. In an attempt to more directly examine the interaction of ammonia with tantalum alkyls, Cp*MeTaMe₄ (**3**)³³ was exposed to ~4 equiv of NH₃. After 2 days in benzene at 100 °C, an uptake of 1.1 (1) equiv of NH₃ was noted, methane was generated (3.1 (1) equiv), and yellow [Cp*MeTaN]₃ (**4**) was isolated in good yield (90%; eq 8). Fewer



equivalents of ammonia generated a complex array of products, as observed by ¹H NMR spectroscopy. Apparently, a substantial excess of NH₃ is needed to break up oligomeric products via

- (19) Babad-Zakhryapin, A. A.; Lagutkin, M. E.; Yushina, L. R. *Izv. Akad. Nauk SSR, Neorg. Mater.* **1974**, *12*, 1130.
 (20) Samsonov, G. V.; Alekseevskii, V. P.; Beletskii, Yu. I.; Pan, V. M.; Timofeev, I. I.; Shvedova, L. K.; Yarosh, V. V. *Issled. Nitridov* **1975**, 219-223.
 (21) Matsumoto, O.; Konuma, M.; Kanzaki, Y. *J. Less-Common Met.* **1978**, *60*, 147-149.
 (22) Kawada, K.; Oosawa, J.; Suzuki, I.; Kizumi, M. (Mitsubishi Metal Corp.). *Jpn. Kokai Tokkyo Koho JP 63, 201, 006* [88,201,006]; *Chem. Abstr.* **1988**, *109*, 233646z.
 (23) (a) Walsh, P. J.; Hollander, F. J.; Bergman, R. G. *J. Am. Chem. Soc.* **1988**, *110*, 8729-8731. (b) For related ammonolyses of metal hydrides, see: Hillhouse, G. L.; Bercaw, J. E. *J. Am. Chem. Soc.* **1984**, *106*, 5472-5478.
 (24) For related 1,2-eliminations, see: (a) Parkin, G.; Bercaw, J. E. *J. Am. Chem. Soc.* **1989**, *111*, 391-393. (b) Cummins, C. C.; Baxter, S. M.; Wolczanski, P. T. *J. Am. Chem. Soc.* **1988**, *110*, 8731-8733 and references therein.
 (25) Schrock, R. R.; Fellmann, J. D. *J. Am. Chem. Soc.* **1978**, *100*, 3359-3370.
 (26) The orange solid precipitated after ~2 days at 20 °C and was thermolized at 100 °C to ensure the maximum uptake of NH₃.
 (27) The combustion analyses may not be wholly accurate due to the stability of the nitrides and carbides of tantalum. In this instance, the nitrogen and hydrogen percentages are reproducible, but substantial scatter was encountered when analyzing for carbon. The value stated represents an average.
 (28) Attempts to analyze these solids via solid-state NMR are ongoing.

- (29) *Powder Diffraction File*; International Centre for Diffraction Data: Swarthmore, PA, 1988.
 (30) The specific phase of TaO was not determined. It is likely that dislocations are prevalent in the crystalline TaN; hence, the TaO probably results from exposure to air.
 (31) (a) Gatterer, J.; Dufek, G.; Etmeyer, P.; Kieffer, R. *Monatsh. Chem.* **1975**, *106*, 1137-1147. (b) Petrunin, V. F.; Sorokin, N. I. *Izv. Akad. Nauk SSR, Neorg. Mater.* **1982**, *18*, 2005-2008.
 (32) The green-orange solid precipitated after 18 h at 20 °C did not appear to undergo further reaction during the 80 °C annealing period (11 h).
 (33) (a) Wood, C. D.; Schrock, R. R. *J. Am. Chem. Soc.* **1979**, *101*, 5421-5422. (b) Mayer, J. M.; Bercaw, J. E. *J. Am. Chem. Soc.* **1982**, *104*, 2157-2165. (c) Sanner, R. D.; Carter, S. T.; Burton, W. J. *J. Organomet. Chem.* **1982**, *240*, 157-162.

Table I. Selected Interatomic Distances (Å) and Angles (deg) for [Cp*MeTaN]₃ (4)^a

Ta1-N1	1.869 (10)	Ta1-N3	1.883 (8)	Ta2-N2	1.878 (9)
Ta2-N1	1.917 (10)	Ta3-N3	1.874 (9)	Ta3-N2	1.892 (9)
Ta1-C1	2.178 (11)	Ta2-C2	2.186 (11)	Ta3-C3	2.170 (13)
Ta1-R1	2.164	Ta2-R2	2.150	Ta3-R3	2.199
N1-Ta1-N3	112.2 (4)	N1-Ta1-N2	111.7 (4)	N2-Ta3-N3	112.6 (4)
Ta1-N1-Ta2	125.9 (5)	Ta2-N2-Ta3	127.2 (5)	Ta1-N3-Ta3	127.3 (5)
N1-Ta1-C1	102.7 (4)	N3-Ta1-C1	100.1 (4)	N1-Ta2-C2	99.7 (5)
N2-Ta2-C2	101.7 (4)	N2-Ta3-C3	102.3 (4)	N3-Ta3-C3	100.5 (5)
C1-Ta1-R1	107.8	C2-Ta2-R2	109.3	C3-Ta3-R3	113.1
N1-Ta1-R1	117.8	N3-Ta1-R1	113.1	N1-Ta2-R2	120.5
N2-Ta2-R2	111.0	N2-Ta3-R3	112.7	N3-Ta3-R3	114.3

^aR1, R2, and R3 are the Cp* ring centroids of C10–C14, C20–C24, and C30–C34, respectively. The ring containing C30–C34 and C35–C39 represents one of two connectivities that model a disorder.

ammonolysis of bridging amide or imide linkages. In accord with this explanation, a complicated set of intermediates emerges and then diminishes during the course of reaction. NMR data (benzene-*d*₆) for **4** manifested complementary sets of Cp* (¹H δ 1.98, 1.97; ¹³C δ 11.24, 10.99, 115.98, 116.01) and Me (¹H δ 0.18, 0.06; ¹³C δ 27.33, 29.83) resonances in 2:1 ratios while molecular weight measurements were consistent with the generation of a trimeric trinitride. ¹⁵N NMR spectra of [Cp*MeTa¹⁵N]₃ (**4**-[¹⁵N₃]), prepared from **3** and ¹⁵NH₃ (98% ¹⁵N), similarly showed two resonances at δ 147.4 and 144.6 (benzene-*d*₆) relative to external CH₃NO₂ (δ 0.0).^{34,35} The infrared spectrum of **4** displayed a strong absorption at 960 cm⁻¹ that was attributed to a TaNTa stretch, since the band in **4**-[¹⁵N₃] shifted to 933 cm⁻¹ (predicted for ν(Ta¹⁵N₃Ta): 930 cm⁻¹).^{14,15} Trimer **4** was thermally stable to 200 °C in benzene, even in the presence of excess NH₃, and no evidence of nitrogen exchange with ¹⁵NH₃ was obtained after 30 days at 100 °C.

In total, the spectroscopic and molecular weight data alluded to the formation of a six-membered [TaN]₃ ring containing two Cp* groups and a Me on one side. Evidence for a C_{3v} isomer possessing all Cp* groups on one side has not been obtained. In a theoretical study of transition-metal nitrides, Wheeler et al.^{36,37} suggested that certain cyclic [MN]₃ species may exist as benzene analogues akin to [X₂PN]₃ phosphazenes.^{38–41} Delocalization of π electrons occupying in-plane orbitals may stabilize a symmetric ring structure relative to one containing alternating long (Ta–N) and short (Ta=N) bonds. The latter situation is favored when this distortion induces substantial mixing between critical occupied and unoccupied orbitals, resulting in localization of π-electron density.⁴² An alternating bond arrangement would render each Ta center of **4** different, resulting in inequivalent Cp*, Me, and N groups, as required by C₁ symmetry. Since the spectroscopic data supports the existence of a mirror plane, the delocalized C_s structure is preferred, yet the possibility of acci-

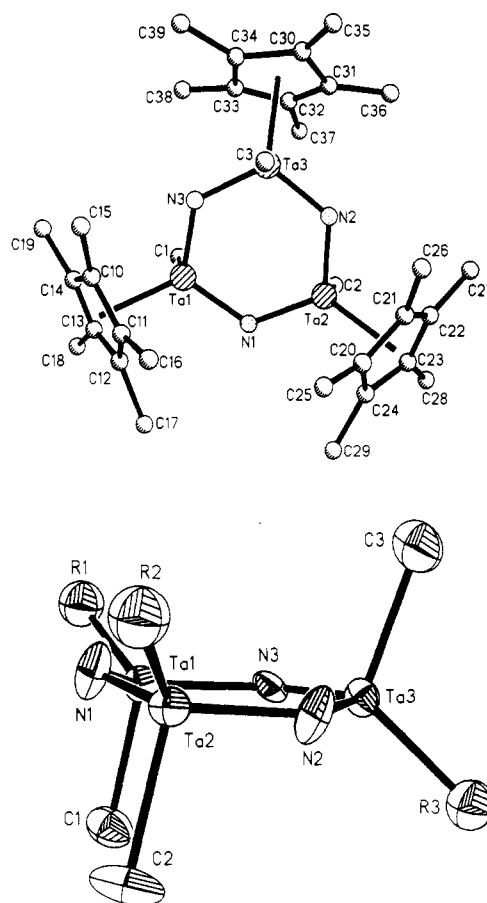


Figure 1. Molecular structure and skeletal view of [Cp*MeTaN]₃ (**4**). R1, R2, and R3 are the Cp* ring centroids of C10–C14, C20–C24, and C30–C34, respectively. The ring containing C30–C34 and C35–C39 represents one of two connectivities that model a disorder.

Table II. Crystallographic Data for [Cp*MeTaN]₃ (**4**)

formula: H ₅₄ C ₃₃ N ₃ Ta ₃	fw = 1035.66
a = 16.951 (5) Å	space group: P2 ₁ /c (No. 14)
b = 8.920 (3) Å	T = -100 °C
c = 23.141 (6) Å	λ = 0.71073 Å (Mo Kα)
β = 91.47 (2)°	ρ _{calc} = 1.967 g cm ⁻³
V = 3498 (2) Å ³	μ = 92.79 cm ⁻¹
Z = 4	

R = 0.057, R_w = 0.098, and GOF = 1.08 where w⁻¹ = σ²(F) + 0.0071F²
R = 0.058, R_w = 0.055, and GOF = 5.20 where w⁻¹ = σ²(F)

dental degeneracies in such closely related fragments cannot be dismissed. IR absorptions pertaining to the linear μ-N bridges of [X₅TaNTaX₅]³⁻ (X = Br, 985 cm⁻¹;⁴³ I, 934 cm⁻¹)⁴⁴ are comparable to the 960-cm⁻¹ band of **4**. Furthermore, the nitrido

- (34) (a) von Philipsborn, W.; Muller, R. *Angew. Chem., Int. Ed. Engl.* **1986**, *25*, 383–406. (b) Mason, J. *Chem. Rev.* **1981**, *81*, 205–227.
- (35) Godemeyer, T.; Dehnicke, K.; Fluck, E. *Z. Anorg. Allg. Chem.* **1988**, *565*, 41–46.
- (36) Wheeler, R. A.; Hoffmann, R.; Strähle, J. *J. Am. Chem. Soc.* **1986**, *108*, 5381–5387 and references therein.
- (37) Wheeler, R. A.; Whangbo, M.-H.; Hughbanks, T.; Hoffmann, R.; Burdett, J. K.; Albright, T. A. *J. Am. Chem. Soc.* **1986**, *108*, 2222–2236.
- (38) (a) Allcock, H. R. *Chem. Rev.* **1972**, *72*, 315–356. (b) Allcock, H. R.; Desorcie, J. L.; Riding, G. H. *Polyhedron* **1987**, *6*, 119–157.
- (39) Neilson, R. H.; Wisian-Nielson, P. *Chem. Rev.* **1988**, *88*, 541–562.
- (40) For transition-metal-substituted cyclic phosphazenes, see: (a) Katti, K. V.; Roesky, H. W.; Tietzel, M. *Inorg. Chem.* **1987**, *26*, 4032–4035. (b) Katti, K. V.; Seseke, U.; Roesky, H. W. *Inorg. Chem.* **1987**, *26*, 814–816. (c) Roesky, H. W.; Katti, K. W.; Seseke, U.; Schmidt, H. G.; Egert, E.; Herbst, R.; Sheldrick, G. M. *J. Chem. Soc., Dalton Trans.* **1987**, 847–849. (d) Roesky, H. W.; Katti, K. W.; Seseke, U.; Witt, M.; Egert, E.; Herbst, R.; Sheldrick, G. M. *Angew. Chem., Int. Ed. Engl.* **1986**, *25*, 477–478. (e) Roesky, H. W. *Polyhedron* **1989**, *8*, 1729–1731. (f) Witt, M.; Roesky, H. W. *Polyhedron* **1989**, *8*, 1736–1741.
- (41) For related transition-metal complexes, see: (a) Roesky, H. W. *Chem. Soc. Rev.* **1986**, *15*, 309–334. (b) Roesky, H. W.; Bai, Y.; Noltemeyer, M. *Angew. Chem.* **1989**, *101*, 788–789.
- (42) Albright, T. A.; Burdett, J. K.; Whangbo, M.-H. *Orbital Interactions in Chemistry*; John Wiley: New York, 1984.

- (43) Frank, K.-P.; Strähle, J.; Weidlein, J. *Z. Naturforsch.* **1980**, *35B*, 300–306.
- (44) Hörner, M.; Frank, K.-P.; Strähle, J. *Z. Naturforsch.* **1986**, *41B*, 423–428.

absorption of structurally characterized $[\text{Cp}^*\text{ClTaN}]_3$, a C_3 complex displaying one type of TaN bond,⁴⁵ is also 960 cm^{-1} . The latter, prepared from Cp^*TaCl_4 and $\text{N}(\text{SnMe}_3)_3$ by Roesky and co-workers, is the first transition-metal example of a delocalized six-membered ring and is directly analogous to **4**. In order to corroborate and understand the presumed similar geometry of **4**, X-ray structural and extended Hückel molecular orbital (EHMO)⁴⁶ studies were undertaken.

X-ray Structure of $[\text{Cp}^*\text{MeTaN}]_3$ (4**).** A single-crystal X-ray structure determination of $[\text{Cp}^*\text{MeTaN}]_3$ (**4**) confirmed its trimeric nature, as illustrated in Figure 1 (monoclinic, $P2_1/c$, $R = 0.057$, $R_w = 0.098$, 5787 (93%) observed reflections where $F \geq 3.0\sigma(F)$). Trimer **4** consists of a slightly puckered six-membered ring with one Me and two Cp^* groups on one side and the complement on the other. Solution via heavy-atom methods proved routine except for the unique Cp^* ring, which was modeled as two separate connectivities, each composed of carbons having 50% occupancy. Six nearly equivalent TaN distances are observed, supporting a delocalized, benzene-like depiction of **4** that has noncrystallographic C_3 symmetry. The only significant deviation ($\sim 2\sigma$) from the average TaN distance ($d(\text{TaN})_{\text{av}} = 1.886$ (17) Å) occurs at Ta2–N1 (1.917 (10) Å), and it coincides with a relatively short Ta1–N1 distance (1.869 (10) Å). This appears to be a local aberration, since the Ta1–N1–Ta2 link is responsible for the ring pucker; N1 deviates significantly (0.295 Å) from the plane defined by Ta1, N3, Ta3, N2, and Ta1 ($\sigma = 0.0285$ Å).^{47,48} Examination of the N–Ta–ring centroid (R) angles ($\angle\text{R1(2)–TaN1}_{\text{av}} = 119.2$ (19)°) shows that the repulsive steric interactions of the cis- Cp^* ligands attached to Ta1 and Ta2 cause N1 to move out of the plane in order to retain near-tetrahedral geometry about the metals. As a result, the Cp^* ligands are also moved closer to their respective methyl groups ($\angle\text{R1(2)TaCl(2)}_{\text{av}} = 108.5$ (11)°; $\angle\text{R1(2)TaN3(2)}_{\text{av}} = 112.0$ (15)°). These average angles contrast significantly with those pertaining to R(3), the centroid of the mutually trans- Cp^* : $\angle\text{R3Ta}_{\text{av}} = 113.5$ (1)°, $\angle\text{R3TaC3} = 113.1$ (10)°.

The ring angles are quite regular ($\angle\text{NTa}_{\text{av}} = 112.2$ (4)°; $\angle\text{TaNTa}_{\text{av}} = 126.8$ (8)°), but both types deviate significantly from 120°. Although the steric interactions of the Cp^*MeTa moieties would be expected to make the NTaN angles $< 120^\circ$ at the expense of the TaNTa angles, recall that virtually every known bridging nitride is linear;^{14,15} hence, electronic effects also play a role. A typical μ -N linkage gains in-plane bonding as it approaches linearity, but the Cp^*MeTa fragment orbitals are constrained geometrically, thereby preventing a triangular structure containing linear μ -N bridges. The Ta–methyl bond distances are normal ($d(\text{TaC})_{\text{av}} = 2.178$ (8) Å), and the corresponding NTaMe angles ($\angle\text{NTaC(Me)}_{\text{av}} = 101.2$ (12)°) again manifest the steric influence of the Cp^* . The distances and angles pertaining to the permethylated cyclopentadienyl rings are typical, despite a disorder in the Cp^* attached to Ta3 that was routinely modeled.

The general features of $[\text{Cp}^*\text{MeTaN}]_3$ (**4**) parallel the characteristics of the aforementioned chloride derivative synthesized by Roesky et al.,⁴⁵ including the puckered six-membered ring whose angles alternate ($\angle\text{TaNTa} > 120^\circ > \angle\text{NTaN}$). In $[\text{Cp}^*\text{ClTaN}]_3$, the Ta opposite to the out-of-plane nitrogen also deviates slightly, giving rise to a subtle boat conformation.⁴⁷ The corresponding Ta3 in **4** does not exhibit a statistically significant deviation.⁴⁸ Both molecules exhibit TaN distances (1.88 (2) Å average in $[\text{Cp}^*\text{ClTaN}]_3$) that are in range of those comprising the linear nitride bridges of $[\text{X}_5\text{TaNTaX}_5]^{3-}$ ($\text{X} = \text{Br}$, 1.849 (2) Å,⁴³ $\text{X} = \text{I}$, 1.847 (6) Å).⁴⁴ The TaN links can be classified as

double bonds, according to Wheeler et al., given that triply bonded Ta imido units usually range from 1.61 to 1.78 Å.^{15,36,49,50} Tantalum–dialkylamido bonds, usually considered to manifest substantial $\text{N}(p\pi) \rightarrow \text{Ta}(d\pi)$ interactions, are somewhat longer (1.95–2.03 Å), but alkylamido ligands (e.g., $^t\text{BuNH}$) approach the TaN distance observed in **4**.⁴⁹

EHMO Investigation of $[\text{Cp}^*\text{MeTaN}]_3$ (4'**).** In order to simplify the EHMO calculations, **4** (C_3) was modeled by a trimer, **4'**, containing three cis- Cp ligands. The C_{3v} geometry of **4'** enabled the use of convenient symmetry labels without substantially perturbing the molecular orbitals critical to the ring bonding. Bond distances and angles were taken from the X-ray crystallographic characterization of **4**. As shown in Figures 2 and 3, the molecular orbital diagram of trimer **4'** was constructed by the interaction of a combination of three $[\text{CpTaMe}]^{3+}$ units with a second fragment composed of three N^{3-} ligands. The orbital splittings of the $[\text{CpTaMe}]^{3+}$ unit are characteristic of a $d^0\text{ML}_4$ quasi-octahedral moiety,⁵¹ consistent with a Cp ring occupying three coordination sites. Five orbitals of $[\text{CpTaMe}]^{3+}$ possessing substantial d character are illustrated on the left of the figures. The highest, $3a'$, consists of a mixture of d_{z^2} and $d_{x^2-y^2}$ perturbed by some p_x , while the lowest, $1a'$, is mostly $d_{x^2-y^2}$. Orbitals $2a'$ and $2a''$ are mainly d_{xz} and d_{xy} , respectively, but additional mixing with p_z and p_y results in hybridized orbitals that are directed away from ligands. The remaining orbital, $1a''$, is nearly pure d_{yz} .

Three $[\text{CpTaMe}]^{3+}$ groups are then arranged equidistantly, leading to the triangular C_{3v} $[\text{CpTaMe}]_3^{9+}$ fragment. Because the Ta...Ta distance is lengthy, the interactions responsible for the $[\text{CpTaMe}]_3^{9+}$ fragment MO's are inherently weak, except those involving orbitals directed between the tantalums. Each combination of like-symmetry $[\text{CpTaMe}]^{3+}$ hybrids results in two types of $[\text{CpTaMe}]_3^{9+}$ fragment orbitals: an a-symmetry MO and an accompanying degenerate e-set. On the right side of each diagram are the nine filled p-orbital combinations of the N_3^{9-} fragment. Generated from equal but distantly spaced N^{3-} ions, these levels manifest little splitting because the atomic orbital interactions are weak, yet the a-below-e energetics is clearly present. The empty $[\text{CpTaMe}]_3^{9+}$ and filled N_3^{9-} fragment orbitals are then mixed in order to construct the diagram corresponding to C_{3v} $[\text{CpMeTaN}]_3$ (**4'**), central to both figures, which separately highlight contributions from out-of-plane (Figure 2) and in-plane (Figure 3) bonding orbitals.

As Figure 2 shows, N^{3-} p_z combinations ($2a_1$, $2e$) contribute to out-of-plane ring bonding by interacting with the $[\text{CpTaMe}]_3^{9+}$ fragment MO's based on the $2a'$ and $1a''$ orbitals of $[\text{CpTaMe}]^{3+}$, because only these have a significant z component ($1e$, $2a_1$, $1a_2$, $4e$). Three filled bonding MO's, a symmetric a_1 and a degenerate e-set, constitute a stable $6e^-$ bonding configuration that resembles the familiar π -bonding MO picture of benzene. The e level and its antibonding partner result from mixing with a linear combination of Ta-based orbitals oriented along the Ta–N line ($1e$), while another ($4e$) remains basically nonbonding. Note that the $1a_2$ orbital is of the wrong symmetry to interact with the out-of-plane N_3^{9-} orbitals and becomes the nonbonding LUMO of **4'**. The remaining energy levels boxed by the dashed lines comprise various Cp- and Me-based MO's that have minimal contribution to the $[\text{TaN}]_3$ -ring bonding.

Figure 3 manifests the in-plane bonding of the six-membered tantalum nitride ring. Here the remaining N_3^{9-} p_x - and p_y -based

(45) Plenio, H.; Roesky, H. W.; Noltemeyer, M.; Sheldrick, G. M. *Angew. Chem., Int. Ed. Engl.* **1988**, *27*, 1330–1331.

(46) Hoffmann, R. J. *Chem. Phys.* **1963**, *39*, 1397–1412 and references therein.

(47) In $[\text{Cp}^*\text{ClTaN}]_3$, the N between the cis- Cp^*ClTa fragments deviates 0.39 Å above the four-atom plane ($\sigma = 0.0003$ Å) defined by all but the opposite Ta, which is also above the plane by 0.13 Å.

(48) For a plane defined by Ta1, Ta2, N2 and N3 ($\sigma = 0.0293$ Å), N1 deviates above the plane by 0.2757 Å, but Ta3 is above by only 0.0607 Å ($\sim 2\sigma$), a deviation that is statistically insignificant. Note that σ for the five-atom plane containing Ta3 is 0.0285 Å.

(49) The shortest imido bonds are reported for related six-coordinate Ta complexes: (a) Jones, T. C.; Nielson, A. J.; Ricard, C. E. F. *J. Chem. Soc., Chem. Commun.* **1984**, 205–206 ($[(^t\text{BuNH})(^t\text{BuNH}_2)\text{ClTa}=\text{N}^t\text{Bu}]_2(\mu\text{-Cl})_2$, imido 1.61 (3) Å, amido 1.86 (3) Å). (b) Bates, P. A.; Nielson, A. J.; Waters, J. M. *Polyhedron* **1985**, *4*, 1391–1401 and references therein ($[(^t\text{BuNH}_2)\text{Cl}_2\text{Ta}=\text{N}^t\text{Bu}]_2(\mu\text{-OMe})_2$, imido 1.70 (2) Å), and references therein.

(50) Hydrazido (Ta=N–N=Ta) bridges are exceptions: (a) Churchill, M. R.; Wasserman, H. J. *Inorg. Chem.* **1981**, *20*, 2899–2904 ($[(\text{Me}_3\text{P})_2\text{NpTa}=\text{CH}^t\text{Bu}]_2(\mu\text{-N}_2)$, 1.840 (8) Å). (b) Churchill, M. R.; Wasserman, H. J. *Inorg. Chem.* **1982**, *21*, 218–222 ($[(\text{PhCH}_2)_3\text{P}](\text{THF})\text{TaCl}_2(\mu\text{-N}_2)$, 1.796 (5) Å).

(51) (a) Elian, M.; Hoffmann, R. *Inorg. Chem.* **1975**, *14*, 1058–1076. (b) Albricht, T. A. *Tetrahedron* **1982**, *38*, 1339–1388.

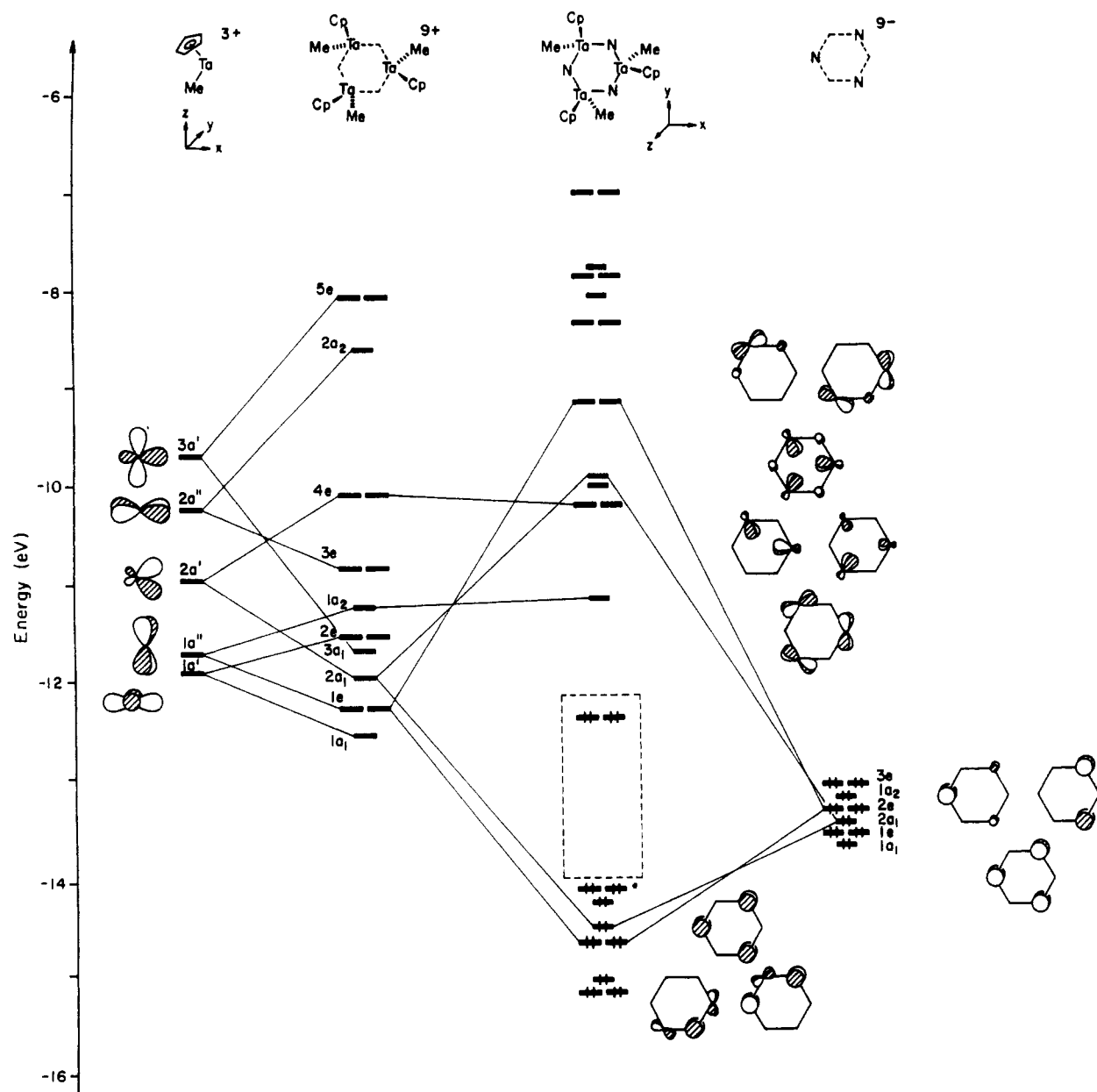


Figure 2. Molecular orbital diagram of C_{3v} $[\text{CpMeTaN}]_3$ (**4**), modeling **4**. Illustrated are the out-of-plane orbitals critical to ring bonding.

orbitals interact with the Ta-localized MO's that are directed into the ring plane, those derived from the $1a'$ and $2a''$ orbitals of $[\text{CpTaMe}]^{3+}$. In this depiction, interactions due to the $3a_1$ and $5e$ levels of $[\text{CpTaMe}]_3^{9+}$ have been neglected because they exhibit minimal overlap with appropriate N_3^{9-} orbitals. Six filled bonding and six empty antibonding molecular orbitals result from these interactions, thereby constituting strong in-plane bonding, which can be described as both σ and $d\pi$, depending on the MO. Again, these MO's can be directly compared with similar in-plane benzene orbitals derived from combining six sp^2 -CH hybrids. The EHMO calculations render overlap populations of 0.781 for the in-plane and 0.460 for the out-of-plane interactions, as expected since twice as many in-plane combinations exist. This situation may be regarded as analogous to the six σ -bonds versus three π -bonds in benzene. Also evident is a substantial amount of electron transfer to formally empty $[\text{CpTaMe}]_3^{9+}$ energy levels; hence, the calculations support covalent bonding with considerable delocalization.

As stated previously, significant mixing between the occupied and unoccupied orbitals can result in a lower energy structure associated with localized TaN double bonds.³⁶ If bond alternation is introduced in **4'**, a slight decrease in energy is noted. Obviously, in this instance the EHMO calculations are unreliable; in general, arguments based on the calculated total energy of bond isomers

are tenuous. Wheeler et al. have concluded that bond alternation exists in cases where the orbitals involved in mixing are energetically close (~ 1 eV).³⁶ Although the HOMO-LUMO gap for **4'** is only ~ 1.2 eV, neither orbital is involved in $[\text{Ta}_3\text{N}_3]$ bonding. However, the out-of-plane, nonbonding LUMO is of a_2 symmetry. A distortion leading to TaN bond alternation would change the point group, allowing a_1 - and a_2 -labeled orbitals in C_{3v} to mix as a -types in C_3 . A crucial interaction between the totally symmetric a_1 out-of-plane bonding orbital and the a_2 LUMO is turned on when the symmetry is lowered. This is precisely the interaction that dictates whether distortion will occur. In **4'**, the energy difference between these two MO's is >3.3 eV; thus, *no substantial mixing should occur, and the trimer is predicted to be symmetric*. Although $[\text{Cp}^*\text{MeTaN}]_3$ (**4**) possesses true C_3 symmetry, a similar type of mixing between orbitals closely resembling those in the C_{3v} model occurs when the mirror plane is removed. Again the critical energy gap is of too great a magnitude; hence, the regular structure prevails.

Curiously, equivalent bond distances in complexes akin to $[\text{Cp}^*\text{MeTaN}]_3$ (**4**) are usually taken as an indication of electron delocalization. In benzene, where all six CH fragments are equivalent, this is certainly the case, but in **4**, the concept of electron delocalization leading to a regular structure may be somewhat misleading. The great energy disparity between the

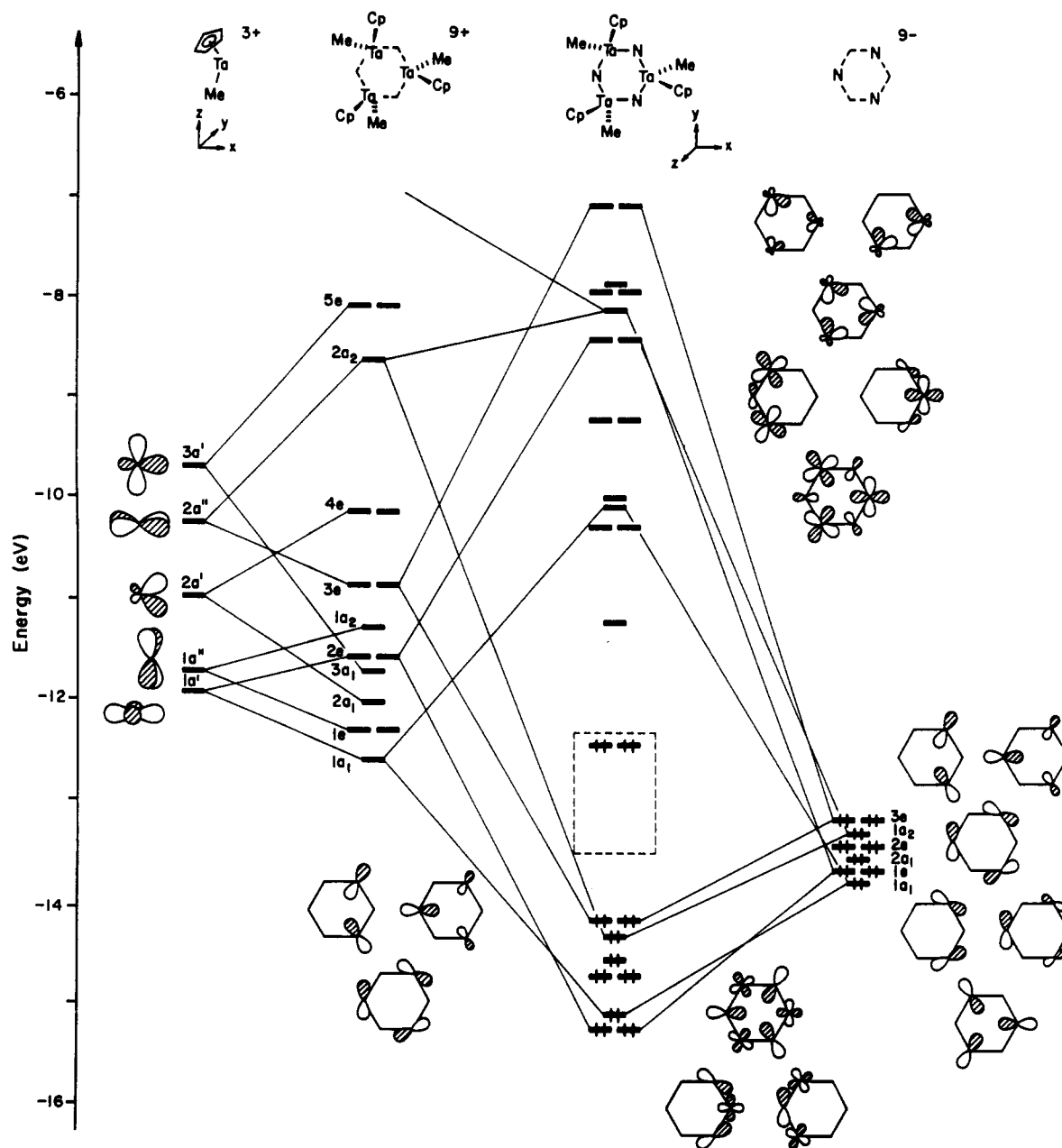


Figure 3. Molecular orbital diagram of C_{3v} $[\text{Cp}^*\text{MeTaN}]_3$ (**4'**), modeling **4**. Illustrated are the in-plane orbitals critical to ring bonding.

LUMO and the out-of-plane a_1 orbital is a direct consequence of the group electronegativity differences between N_3^{9-} and $[\text{Cp}^*\text{TaMe}]_3^{9+}$; hence, it can be argued that the *localization* of charge on the N_3^{9-} fragment is responsible for equivalent TaN bond distances. As mentioned previously, the calculations do seem to reflect significant π -electron delocalization into the $[\text{Cp}^*\text{TaMe}]_3^{9+}$ units, but the pictorial representation of the bonding orbitals in the figures belies this observation. In questions of charge distribution, the EHMO method may underestimate ionic contributions to the bonding.

Reduction of $[\text{Cp}^*\text{MeTaN}]_3$ (4**).** The predicted existence of a nonbonding LUMO of **4'** residing only ~ 1.2 eV above the HOMO prompted attempts to reduce $[\text{Cp}^*\text{MeTaN}]_3$ (**4**). Figure 4 illustrates the cyclic voltammogram (CV) of **4** in THF with 0.1 M $[\text{nBu}_4\text{N}][\text{BF}_4]$ as the added electrolyte. The reduction observed at -2.7 V vs NHE (~ -2.1 V vs Ag wire) was shown to be electrochemically reversible at various scan speeds (10–500 mV/s). Coulometry revealed that 0.97 (3) e was passed per mole of **4**, consistent with the peak separation of 59 mV (50 mV/s, $i_{pc}/i_{pa} = 1.00$ (2), corrected for IR drop) in the CV,⁵² indicating a

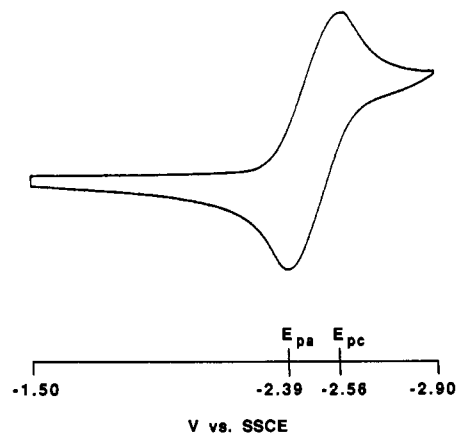


Figure 4. Cyclic voltammogram (CV) of $[\text{Cp}^*\text{MeTaN}]_3$ (**4**) showing the reversible formation of $[\text{Cp}^*\text{MeTaN}]_3^-$ (**5**): conventional cell; 0.0011 M **4**, 0.1 M nBu_4NBF_4 ; working and counter electrodes, Pt; reference electrode, SSCE; sweep rate, 100 mV/s.

chemically reversible 1-e process. During the coulometry experiments, the initial yellow solution turned a deep purple color

(52) Bard, A. J.; Faulkner, L. R. *Electrochemical Methods: Fundamentals and Applications*; Wiley: New York, 1980.

ammonolysis studies of early-transition-metal alkyls, alkoxides, amides and difunctionalized metal precursors are also ongoing.

Experimental Section

General Considerations. All manipulations were performed with use of either glovebox or high-vacuum-line techniques. Etheral and hydrocarbon solvents were distilled under nitrogen from purple benzophenone ketyl and vacuum transferred from the same prior to use. Small amounts of tetraglyme (2–5 mL/mL solvent) were added to hydrocarbons to solubilize the ketyl. Benzene- d_6 was dried over activated 4-Å molecular sieves, vacuum transferred, and stored under N_2 ; THF- d_8 was dried over sodium benzophenone ketyl. Anhydrous ammonia was purchased from Matheson and distilled from sodium. $^{15}NH_3$ was used as purchased from Aldrich. Electrometric grade nBu_4NBF_4 was purchased from Southwestern Analytical Chemicals, recrystallized three times from ethyl acetate/ether, and dried in vacuo. $(^nBuCH_2)_3Ta=CH^tBu$ (**1**)²⁵ and Cp^*TaMe_4 (**3**)³³ were prepared via literature procedures. The argon in the furnace flow system was scrubbed by a Nanochem Gas Purifier (Model L-30t, Hercules) and by a piece of Ti foil placed in a crucible upstream of the sample.

NMR spectra were obtained by using Varian XL-200 (1H) and XL-400 (1H , $^{13}C\{^1H\}$, ^{15}N) spectrometers. Chemical shifts are reported relative to TMS (1H) or benzene- d_6 (1H , δ 7.15; $^{13}C\{^1H\}$, δ 128.00). ^{15}N spectra were referenced to natural abundance CH_3NO_2 (neat, δ 0.00)^{34,35} by using a coaxial 5 mm tube containing the lock solvent; a delay of 40 s and a pulse width of 30° were employed. Infrared spectra were recorded on a Mattson FT-IR instrument interfaced to a AT&T PC7300 computer. Molecular weights were obtained on a home-built device for benzene cryoscopy.⁵⁹ Cyclic voltammograms were performed with an IBM EC/225 voltammeter and Soltec VP-6423S XY recorder. A silver-wire reference electrode or sodium-saturated calomel reference electrode, a platinum-wire counter electrode, and a platinum working electrode (0.0096 cm²) were employed. Coulometry was performed by using a Princeton Applied Research Model 173 potentiostat fitted with a Model 179 digital coulometer. A silver wire, a platinum-wire counter electrode, and platinum-gauze working electrode were utilized. Analyses were obtained by Oneida Research Services, Whitesboro, NY. X-ray powder patterns were taken with a Scintag XDS 2000 diffractometer and samples were referenced to the Powder Diffraction File.²⁹

Procedures. **1a. Synthesis of $1/n[(H_2N)_a(HN)_b(N)_cTa(CH_2^tBu)_{(5-(a+2b+3c))}]_n$ (**2**).** A glass bomb was charged with 1.249 g (2.689 mmol) of $(^nBuCH_2)_3Ta=CH^tBu$ (**1**) and evacuated and 50 mL of benzene introduced by distillation. Ammonia (13.5 mmol, 5.0 equiv) was measured out in a calibrated gas bulb and condensed into the reaction vessel at $-198^\circ C$. The bomb was covered with aluminum foil to exclude light and the solution stirred 2 days at $23^\circ C$. The stirred mixture was then heated to $100^\circ C$ for 2 days. Upon cooling to $23^\circ C$, a clear, colorless solution and fine orange solid were present. Filtration of the solid and subsequent washing with hexane gave 0.453 g of an orange powder (**2**). Anal. Found (av): C, 1.53; H, 0.91; N, 13.89.

1b. NH_3 Uptake. The reaction mixture contained in the bomb reactor from procedure 1 was cooled to $-18^\circ C$ and the residual gas condensed into 25 mL of degassed aqueous HCL (2.907 M). This process was repeated four times to ensure transfer of all NH_3 . Two 10.00 (2)-mL aliquots of the resulting solution were then titrated with standardized NaOH (0.9448 M) with phenolphthalein used as indicator.

1c. Neopentane Loss from **1.** An NMR tube sealed to a ∇ 14/20 joint was charged with 21 mg (0.045 mmol) of **1** and 19 mg (0.102 (5) mmol) of Cp_2Fe . Ammonia (0.229 mmol, 5.2 equiv) was measured in a calibrated gas bulb and condensed into the tube at $-198^\circ C$. The tube was flame-sealed. The amount of neopentane present in solution was then determined via integration of the peaks by 1H NMR spectroscopy, with ferrocene used as the internal standard.

2. TaN from **2.** An alumina boat was charged with 0.125 g of **2**. The boat was placed inside a quartz tube fitted with stainless-steel end pieces and the solid heated in a split-furnace under flowing argon. The orange solid turned black by $400^\circ C$ and remained black as the furnace was heated to $820^\circ C$. The yields of material were 0.118 g at $400^\circ C$ (~6% weight loss) and 0.116 g at $820^\circ C$. The jet-black solid became gray upon exposure to air. X-ray powder diffraction studies indicated that the sample was ~95% cubic ($Fm\bar{3}m$) TaN and ~5% TaO.³⁰ At temperatures $>900^\circ C$ (3 days), TaN_{0.8} was observed to grow in with a corresponding weight loss.

3. Synthesis of **2' under Ambient Light.** Procedures 1a–c and 2 were used except that the solution was exposed to ambient light for 18 h at $20^\circ C$ and then heated for 11 h at $80^\circ C$. Data for a typical run are as follows: 1.222 g of **1** (2.631 mmol); 2.0 equiv of NH_3 (5.26 mmol);

uptake of NH_3 was 1.53 equiv; 3.7 equiv of neopentane lost; 0.553 g of green orange **2'** isolated. Anal. Found: C, 7.41; H, 1.72; N, 11.65. Thermolysis of **2'** (0.130 g) at $400^\circ C$ for 24 h produced 0.112 g (~14%) of an amorphous black powder. Annealing at $820^\circ C$ (3 days) produced a jet-black solid (0.110 g), identified by X-ray powder diffraction as cubic TaN ($Fm\bar{3}m$ $a = 4.300$ (2) Å), that was not affected by exposure to air.

4. $[Cp^*MeTaN]_3$ (4**).** A glass bomb reactor with a Teflon valve was charged with 1.41 g (3.75 mmol) of Cp^*TaMe_4 and a stir bar. Benzene (20 mL) and 15.0 mmol (4.0 equiv) of ammonia were condensed into the bomb at $-198^\circ C$. With the apparatus behind a safety shield, the stirred mixture was heated to $100^\circ C$ for 2 days, resulting in a clear yellow solution. An uptake of 1.1 (1) equiv of NH_3 was noted concomitant with the generation of 3.1 (1) equiv of methane (Toepler pump). A fine yellow solid was isolated by filtration from hexanes (1.163 g, 90%). The ^{15}N -labeled material was prepared in the same manner by utilizing $^{15}NH_3$. 1H NMR (C_6D_6): δ 0.06 (s, Me, 3 H), 0.18 (s, Me, 6 H), 1.97 (s, Cp*, 15 H), 1.98 (s, Cp*, 30 H). ^{13}C NMR (C_6D_6): δ 10.99, 11.24 (Cp*, $\sim 1:2$), 27.33, 29.83 (TaCH₃, $\sim 2:1$), 115.98, 116.01 (CH₃(Cp*), $\sim 2:1$). ^{15}N NMR (C_6D_6): δ 144.6, 147.4 ($\sim 1:2$). IR (Nujol): $\nu(TaN-Ta)/\nu-Ta^{15}NTa = 960/933$ cm⁻¹. M_r : found 1058 (calcd 1036). MS (FABS, He, Nujol matrix): found 1035.1 (M⁺), 1036.1 ((M + 1)⁺); calcd 1035.66 (M⁺). Anal. Calcd for C₃₃N₃H₅₄Ta₃: C, 38.27; H, 5.26; N, 4.06. Found: C, 38.44; H, 5.23; N, 3.86.

5a. Synthesis of $[K\cdot Et_2O]^+[[Cp^*MeTaN]_3]^-$ (5**).** A 25-mL flask containing 2.2 equiv of Na/K (22 mg of Na/44 mg of K) was charged with 520 mg (0.502 mmol) of **4** and a glass stir bar. Et₂O (20 mL) was added at $-78^\circ C$ and the solution allowed to warm to $23^\circ C$ while being rapidly stirred, resulting in an intense royal purple solution. After 90 min, the solution was filtered and the ether stripped, giving 482 mg (83%) of thermally sensitive **5** as a deep purple solid. The anion may be stored at $-20^\circ C$ for weeks with minor decomposition. 1H NMR (**5**, THF- d_6): δ ~15 (Me, $\nu_{1/2} = 300$ Hz), ~22 (Cp*, $\nu_{1/2} = 500$ Hz). 1H NMR ($[K(18-crown-6)]^+[[Cp^*MeTaN]_3]^-$ (**5'**): δ ~19 (Me, $\nu_{1/2} = 160$ Hz), ~22 (Cp*, $\nu_{1/2} = 440$ Hz). The assignments are tentative, since the shifts and widths are dependent upon how much **4** is present.⁵⁵ Approximately 10% impurities are also observed, both diamagnetic and paramagnetic. IR (nujol): $\nu(TaN-Ta) = 964$ cm⁻¹. EPR (THF- d_6): at $-175^\circ C$, $g = 1.97$, $\Delta H = 250$ G; at $-70^\circ C$, $\Delta H = 450$ G.

5b. Oxidation of **5.** An NMR tube sealed to a ∇ 14/20 joint was charged with 41 mg (0.036 mmol) of **5** and 12 mg (0.036 mmol) of $Cp_2Fe^+PF_6^-$. One milliliter of THF was distilled into the tube and the resulting brown solution agitated for 15 min. The THF was stripped, and benzene- d_6 was distilled into the tube, which was then flame-sealed. The experiment was also performed in an identical manner with $AgBF_4$ as the oxidant. Determination of the relative product percentages was determined by 1H NMR spectroscopy, using ferrocene as an internal standard.

Physical Studies. 1. Cyclic Voltammetry of **4.** A three-compartment cell partitioned by fritted glass disks was charged with 0.1 M nBu_4NBF_4 in the side compartments and 1.06×10^{-3} M THF solution of **4** containing 0.1 M nBu_4NBF_4 in the center compartment. The working electrode, counter electrode, and the holder for the SSCE reference electrode were fitted to the cell. Parafilm was then utilized to seal all joints and cover the holder for the reference electrode. The cell was removed from the inert-atmosphere drybox and the SSCE electrode placed in a side compartment of the cell, puncturing the parafilm seal. Cyclic voltammetry was promptly carried out. Alternatively, a silver wire was used as the reference electrode, and all manipulations were performed in the inert atmosphere box. The latter technique was used to study the effect of sweep rate (10–500 mV/s) on reversibility while the first technique was used to determine $E^{o'}$ = -2.5 V vs SSCE (-2.7 V vs NHE).

2. Coulometry of **4.** A three-compartment cell (partitions consisted of fritted glass) was fitted with the reference and counter electrodes each in a side compartment filled with 0.1 M nBu_4NBF_4 in THF. The working electrode was placed in the center compartment along with a 1.16×10^{-3} M THF solution of **4** containing 0.1 M nBu_4NBF_4 and a glass stir bar. A preliminary CV was taken to locate $E^{o'}$, and it was found to be -2.1 V vs silver wire. Electrolysis of the stirred solution was performed at -2.5 V and was complete in 30 min, giving a clear, deep purple solution. A CV showed $[Cp^*MeTaN]_3^-$ to be the only electrochemically active species present. The i/t curve indicated clean coulometry. Electrolysis of an identical background without the presence of **4** was also performed.

3. X-ray Crystal Structure of $[Cp^*MeTaN]_3$ (4**).** A yellow, single-crystalline prism of $[Cp^*MeTaN]_3$ (**4**), approximately $0.5 \times 0.25 \times 0.25$ mm, was grown from benzene solution and sealed in a thin-walled Lindemann capillary. Precise lattice constants for a monoclinic cell, determined from a least-squares fit of 15 diffractometer-measured 2θ values, were $a = 16.951$ (5) Å, $b = 8.920$ (3) Å, $c = 23.141$ (6) Å, $\beta = 91.47$ (2)°, $Z = 4$, and $T = -100^\circ C$. The cell volume was 3498 (2) Å³

Table III. Atomic Coordinates ($\times 10^4$) and Equivalent Isotropic U^a ($\text{\AA}^2 \times 10^4$) for $[\text{Cp}^*\text{MeTaN}]_3$ (**4**)

atom	x	y	z	$U(\text{eq})$
Ta1	2427 (1)	1231 (1)	2294 (1)	254 (2)
Ta2	3716 (1)	2098 (1)	1260 (1)	245 (2)
Ta3	1761 (1)	2012 (1)	944 (1)	261 (2)
N1	3413 (6)	1872 (11)	2047 (4)	388 (32)
N2	2835 (5)	2195 (10)	753 (4)	355 (29)
N3	1630 (5)	1499 (10)	1721 (4)	292 (26)
C1	2540 (7)	-1201 (13)	2278 (6)	424 (40)
C2	4154 (7)	-164 (12)	1095 (6)	467 (42)
C3	1373 (7)	4330 (15)	952 (7)	547 (47)
C10	1501 (11)	2396 (30)	2931 (6)	942 (91)
C11	2242 (12)	3140 (14)	3018 (9)	701 (66)
C12	2684 (10)	2209 (33)	3254 (9)	980 (102)
C13	2332 (10)	820 (17)	3347 (6)	594 (51)
C14	1593 (10)	896 (22)	3164 (6)	695 (59)
C15	795 (18)	3128 (48)	2677 (9)	2985 (364)
C16	2427 (23)	4727 (21)	2874 (13)	2981 (292)
C17	3593 (13)	2265 (49)	3469 (10)	3343 (336)
C18	2598 (21)	-542 (32)	3685 (9)	1929 (198)
C19	890 (13)	-191 (37)	3149 (11)	2168 (192)
C20	4275 (7)	4552 (13)	1347 (5)	382 (36)
C21	4121 (7)	4396 (13)	754 (5)	364 (35)
C22	4605 (7)	3284 (14)	540 (5)	436 (39)
C23	5094 (7)	2768 (14)	994 (7)	495 (46)
C24	4883 (7)	3572 (15)	1497 (5)	474 (40)
C25	3911 (10)	5735 (16)	1745 (7)	751 (61)
C26	3545 (10)	5271 (19)	382 (7)	800 (65)
C27	4547 (10)	2806 (17)	-66 (6)	751 (56)
C28	5757 (9)	1674 (21)	950 (10)	952 (78)
C29	5276 (10)	3508 (26)	2102 (7)	1026 (87)
C30	861 (21)	1808 (32)	34 (13)	393 (66)
C31	1573 (11)	853 (23)	-37 (8)	177 (36)
C32	1562 (12)	-319 (24)	363 (10)	145 (39)
C33	915 (16)	-246 (25)	726 (9)	249 (44)
C34	464 (13)	1028 (30)	562 (11)	268 (49)
C35	672 (30)	3030 (49)	-358 (22)	1002 (153)
C36	2200 (18)	936 (37)	-495 (13)	570 (73)
C37	2162 (16)	-1518 (30)	409 (11)	505 (60)
C38	617 (21)	-1206 (36)	1181 (14)	665 (86)
C39	-346 (25)	1441 (50)	819 (19)	1059 (129)
C30'	1219 (23)	1647 (37)	-13 (13)	491 (76)
C31'	1611 (18)	253 (46)	195 (16)	512 (78)
C32'	1246 (25)	-290 (37)	615 (16)	578 (83)
C33'	606 (16)	510 (34)	735 (11)	284 (53)
C34'	582 (13)	1698 (25)	325 (10)	249 (42)
C35'	1578 (26)	2195 (43)	-504 (17)	1026 (112)
C36'	2345 (31)	-256 (59)	-141 (22)	1339 (164)
C37'	1385 (28)	-1632 (48)	939 (20)	1064 (128)
C38'	-33 (22)	330 (44)	1163 (16)	864 (100)
C39'	-58 (24)	3007 (42)	255 (18)	940 (120)

^a Equivalent isotropic U is defined as one-third of the trace of the orthogonalized U_{ij} tensor.

with a calculated density of 1.967 g/cm³. The space group was determined to be $P2_1/c$, and the absorption coefficient ($\mu(\text{Mo K}\alpha)$) was 92.79 cm⁻¹. Diffraction maxima ($h, \pm k, \pm l$) with $3.0^\circ \leq 2\theta \leq 45^\circ$ were measured on a four-circle, computer-controlled diffractometer (Syntex P₂) with variable 2θ - θ scan using graphite-monochromated Mo $K\alpha$ radiation

($\lambda = 0.71073 \text{ \AA}$). After correction for Lorentz, polarization, and background, 5787 (93.3%) of the merged and averaged unique data (6204) were judged observed ($F \geq 3.0\sigma(F)$).⁶⁰ The tantalum positions were calculated from a Patterson synthesis by using the SHELXTL PLUS system. Subsequent Fourier difference maps revealed the Ta-N ring, the methyls attached to the tantalums, and the two Cp* groups on the same side of the ring. Eight peaks were present where the ring carbons of the third Cp* were expected. A rotational disorder was modeled by placing two rigid pentagons at the site and allowing them to refine via least-squares cycles. The site occupancy of the two rings was explored, but did not deviate significantly from 50%. Methyl groups were then fixed to the ring carbons at 1.51 Å, and hydrogens were fixed at 0.96 Å to all methyl groups (riding model, fixed isotropic U). Refinement was carried out by using full-matrix least-squares refinement (minimization of $\sum w(|F_o| - |F_c|)^2$, where w is based on counting statistics modified by an ignorance factor ($w^{-1} = \sigma^2(F) + 0.0071F^2$) of all non-hydrogen atoms except for the disordered Cp* in which all the carbons were left isotropic. The constraints were lifted from the modeled Cp* for the final refinement. At the final stage of refinement, one reflection was rejected because its abnormal intensity did not coincide with that of its Friedel partner. The highest peak in the final difference map was 3.65 e Å⁻³ (0.95 Å from Ta3). The final residuals from 5787 observations and 342 parameters were $R = 0.057$, $R_w = 0.098$, and GOF = 1.08. A different weighting scheme ($w^{-1} = \sigma^2(F)$) yielded $R = 0.058$, $R_w = 0.055$,⁶¹ and GOF = 5.20.

Extended Hückel Calculations. The geometry of C₃₀ [$\text{CpMeTaN}]_3$ (**4'**) was modeled after **4**. EHMO calculations were performed with weighted H_{ij} 's and parameters taken from previous work.⁶² Those for tantalum were as follows: 6s ($H_{ij} = -10.10 \text{ eV}$), 2.28; 6p (-6.86 eV), 2.24; 5d (-12.10 eV), 4.762 (ζ_2), 0.6815 (C_1), 0.5774 (C_2).

Acknowledgment. Primary support from the Air Office of Scientific Research (AFOSR-87-0103) and the Cornell Materials Science Center (NSF) is gratefully acknowledged as are contributions from the Union Carbide Innovation Recognition Program and Cornell University. M.K. is grateful to the Deutscher Akademischer Austauschdienst (DAAD) for the award of a NATO postdoctoral fellowship. We thank Profs. Frank J. DiSalvo and Hector D. Abruña for helpful discussions, and Dr. Paul Krusic and Steve Hill from Du Pont Central Research for aid in the EPR studies. Support for the Cornell NMR Facility from the NIH and NSF instrumentation programs is also acknowledged. We also thank Dr. Andrea E. Martin and Hercules, Inc., for the generous gift of the Nanochem purification system.

Supplementary Material Available: Listings of information pertaining to the X-ray structural investigation of $[\text{Cp}^*\text{MeTaN}]_3$ (**4**), including a summary of crystal data encompassing data collection and solution/refinement, atomic coordinates, hydrogen atom coordinates, isotropic and anisotropic temperature factors, bond lengths, and bond angles (10 pages); a listing for **4** of observed and calculated structure factors (23 pages). Ordering information is given on any current masthead page.

- (60) Cromer, D. T.; Mann, J. B. *Acta Crystallogr., Sect. A* **1968**, *A24*, 321-324.
(61) $R = \sum ||F_o| - |F_c|| / (\sum |F_o|)$; $R_w = \{ \sum w(|F_o| - |F_c|)^2 / \sum w(|F_o|)^2 \}^{1/2}$.
(62) (a) Lauher, J. W.; Hoffmann, R. *J. Am. Chem. Soc.* **1976**, *98*, 1729-1742. (b) Hoffman, D. M.; Hoffmann, R.; Fiesel, C. R. *J. Am. Chem. Soc.* **1982**, *104*, 3858-3875.